Université Scientifique et Médicale de Grenoble

INSTITUT DES SCIENCES NUCLÉAIRES
DE GRENOBLE

53, avenue des Martyrs – GRENOBLE

ISN 83.59
November 1983

NUCLEAR STRUCTURE AT HIGH AND VERY HIGH SPIN THEORETICAL DESCRIPTION

Z. SZYMANSKI

Lectures delivered at Ecole Joliot-Curie de Physique Nucléaire : "Structure nucléaire aux frontières de la stabilité", Bombannes, Sept. 12-16, 1983.

Laboratoire associé à l'Institut National de Physique Nucléaire et de Physique des Particules.

ISN--83-51.

NUCLEAR STRUCTURE AT HIGH AND VERY HIGH SPIN

THEORETICAL DESCRIPTION*

Z. SZYMANSKI**

Institut des Sciences Nucléaires - 53, Avenue des Martyrs , 38026 Grenoble-Cédex, France

Abstract

Chapter I - Classical rotation

When the existence of nuclear shell structure is ignored and nuclear motion is assumed to be classical we may expect that the nuclear rotation resembles that of a liquid drop. Energy of the nucleus can be thus considered as a sum of three terms : surface energy, Coulomb energy and rotational energy. Nuclear moment of inertia is assumed to be that of a rigid-body.

At a slow rotation about a fixed axis the nucleus seems to acquire a slightly oblate shape. An analogous argument has been used long ago by Newton who calculated the deformation of Earth. At a fast rotation the oblate shape of nucleus may become unstable with respect to the triaxial very elongated deformation. This is again analogous to the Jacobi instability discussed in astrophysics. One finds that the same type of instability may settle in not too heavy nuclei. In very heavy nuclei the fission process may occur first before the Jacobi instability can play any role. The results of a calculation of the energy surfaces in rotating nuclei by Cohen,Plasil and Swiatecki are discussed.

Chapter II - Quantal orbits in rotating nuclei

Cranking procedure is analysed as a tool to investigate nucleonic orbits in a rotating nuclear potential. Signature is introduced as a good quantum number in the rotating potential. Energies and alignments in nucleonic orbits are discussed in terms of angular velocity ω. The potential energy surfaces are calculated and discussed for any (fixed) value of angular momentum. They define various regimes of nuclear motion with different symmetries in nuclear shapes and various relative positions of the nuclear symmetry axes with respect to the rotation axis. Some predictions concerning the possible onset of a superdeformed phase are given.

Chapter III - High-spin rotational bands in deformed nuclei

The structure of nuclear rotation is examined in the presence of the short-range pairing forces that generate the superfluid correlations in the nucleus. Examples of the Bengtsson-Frauendorf plots (quasiparticle energies versus angular velocity of rotation) are given and discussed. The backbending phenomenon is analysed in terms of band crossing. The dependence of the crossing frequency on the pairing-force strength is discussed. Possibilities of the role of new components in the two-body force (quadrupole-pairing) are considered. Possibilities of the phase transition from superfluid to normal states in the nucleus are analysed. The role of the second (dynamic) moment of inertia $\mathcal{J}^{(2)}$ in this analysis is discussed.

Chapter IV - Complete alignment in axially symmetric nuclei

In spherical or weakly deformed nuclei (mostly oblate) angular momentum is aligned parallel to the nuclear symmetry axis. Rotation is of non collective origin in this case. The motion is best analysed by representing nuclear single-particle energies as points in the (m,e) plane. States with non zero angular momenta are those that populate levels corresponding to a sloping Fermi surface in the (m,e) plane.

Examples of the analysis of nuclear spectra in this case (exhibiting also the isomeric states called yrast (traps) are given.

Possible forms of the collective excitations superimposed on top of the high-spin states are discussed. In particular, the giant resonance excitations formed on top of the high-spin states are considered and their properties discussed;

---

*Lectures delivered at Ecole Joliot-Curie de Physique Nucléaire, Sept. 1983,Bombannе,France.

**On leave of absence from Institute for Theoretical Physics,University of Warsaw,Poland.

1 . Classical rotation

Considerable changes in nuclear shape may be expected in the state of a fast nuclear rotation. This is actually one of the reasons why nuclear studies of the high-spin states are so interesting. In the preliminary attempt to describe nuclear phenomena, it is reasonable to ignore the existence of nuclear shell structure, the possible influence of particular nuclear orbits etc., i.e. to consider a "macroscopic" description. Moreover, we shall also ignore in this preliminary approach all the possible quantal effects thus limiting ourselves to a classical motion. Let the equation

$$R = R_0 \left\{ 1 + \sum_{\lambda\mu} \beta_{\lambda\mu} \; Y_{\lambda\mu}(\theta,\phi) \right\} \qquad (1)$$

describe a nuclear surface (if anything like a sharp nuclear surface exists; otherwise, we may consider surfaces e.g. of equal density or potential). Deformation parameters $\beta_{\lambda\mu}$ up to $\lambda \leq 3$ and often of even higher multipolarity (β_{40}, β_{50}, β_{60}) have been discussed in literature. We shall limit our discussion to the quadrupole deformations only. We shall also employ a system of axes overlapping with the main axes of the nucleus. We are then left with the two deformation parameters, β_{20} and $\beta_{22} = \beta_{2-2}$. Using another notation

$$\beta_{20} = \beta \cos\gamma \qquad (2)$$

$$\beta_{22} = \beta_{2-2} = \frac{1}{\sqrt{2}} \beta \sin\gamma \qquad (3)$$

we can employ a (β,γ) - plane (β-radial coordinate, γ-angle) as to describe nuclear shape.

Fig. 1 (taken from ref.[1]) illustrates the calculated contour plots of equal energies for a classical rotational motion of a uniformly charged nucleus of a constant density at angular momentum I = 40. Values at $\gamma = -120°$, $-60°$, $0°$ and $60°$ correspond to axially symmetrical shapes (prolate or oblate) corresponding to various orientations of the rotation axis with respect to the symmetry axis as indicated in the figure. The intermediate regions correspond to the rotations of the triaxial shapes about the axis of largest moment of inertia $\mathfrak{I}$ ($0° < \gamma < 60°$), axis of intermediate $\mathfrak{I}$ ($-60° < \gamma < 0°$), or axis of the lowest moment of inertia $\mathfrak{I}$ ($-120° < \gamma < -60°$).

It seems quite natural that the nucleus that is spherical at I = 0, will get oblate for

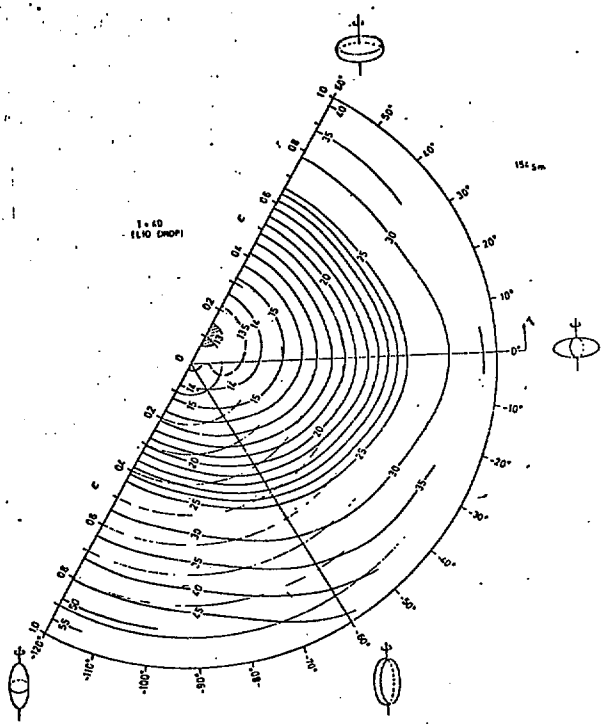

Figure 1

$I \neq 0$. This is quite analogous to the conclusion of Newton who claimed that the Earth is approximately of the shape of an oblate axially symmetric ellipsoid owing to its rotation (Fig. 2). Knowing a gravitational potential of a slightly deformed sphere Newton has calculated the Earth deformation as

$$\beta = \frac{\sqrt{5\pi}}{3} \cdot \frac{\omega^2 R_o}{(\gamma M/R_o^2)} \approx 0.0046 \qquad (4)$$

(here ω denotes the angular velocity, R_o - spherical radius, M - the Earth mass and γ - gravitation constant). The actual value of the Earth deformation is somewhat lower

$$\beta_{exp} \approx 0.0036 \qquad (5)$$

the difference following mainly from the Newton assumption of constant mass density of the Earth (cf. ref.[2]). Nevertheless, Newtons first estimate (4) seems to lie quite close to this value.

However, it is interesting to observe that when the nucleus rotates fast enough the oblate shape may become unstable at certain angular velocity ω with respect to the triaxial and then very elongated shapes. This curious instability which is related to the breaking of axial symmetry was already known long ago to Jacobi (cf. ref.[2]) and has been widely discussed in astrophysics in connection with the equilibrium of rotating stars. Similar situation may occur in principle in a rotating nucleus. However, contrary to the rotating astronomical objects that are hold together by the long-range gravitational forces, in the rotating nuclei we have to deal with the short-range, attractive forces. They may show up in the form of a surface tension of a nuclear "liquid drop". The competition between the surface tension and the centrifugal stretching that acts in the nucleus at a very fast rotation may tend to produce a situation similar to that of the Jacobi instability. The hypothetical very elongated shapes of nuclei that may occur at very fast rotation are often called nuclear superdeformed states. Fig. 3 shows a schematical but very instructive estimate by Mottelson of the balance between surface and rotational energy of a rotating cylinder. In Fig. 3a a very flat cylinder rotates about its symmetry axis while in Fig. 3b a very elongated cylinder rotates about an axis perpendicular to its own symmetry axis. In both cases the sum of surface and rotational energy is minimized for fixed angular momentum I (and for fixed volume). Then, the asymptotic dependence of energy on I is examined. It is seen that in the final account the elongated shape must win over the oblate one since it accomodates better the energy. We can thus expect the Jacobi instability to play an important role in the physics of nucleus at high angular momentum.

The above argument was based on the assumption that the nuclear moment of inertia $\mathcal{I}$ is

Earth deformation (Newton)

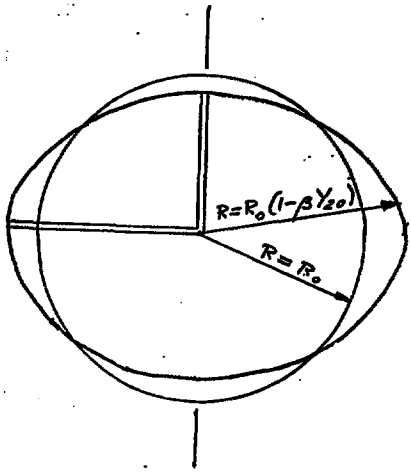

$$\beta = \frac{\sqrt{5\pi}}{3}\,\frac{\Omega^2 R}{\mathcal{G}M/R^2} = 0.00455 \qquad \text{(uniform density)}$$

$$\beta_{exp} = 0.00360$$

Figure 2

Mottelson estimate (a)

$E \sim R^2 + \xi \frac{I^2}{R^2}$

$0 = \frac{dE}{dR} = 2R - \xi \frac{2I^2}{R^3} \Rightarrow R \sim \sqrt{I}$

$E \sim I$

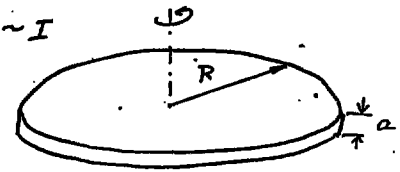

(b)

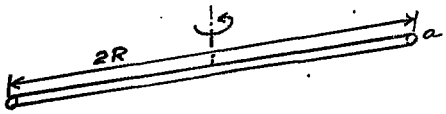

$V \sim a^2 R \Rightarrow S \sim aR \sim \sqrt{R}$

$E \sim \sqrt{R} + \gamma \frac{I^2}{R^2}$

$0 = \frac{dE}{dR} \sim \frac{1}{2\sqrt{R}} - \gamma \frac{2I^2}{R^3} \Rightarrow R \sim I^{4/5}$

$E \sim I^{2/5}$

Figure 3

of the order of the rigid-body value corresponding to the actual nuclear size, deformation and density. This assumption seems to be reasonable in a more general situation and leads to a good description of nuclear rotation. It appears that in the domain of a fast nuclear rotation (when in particular, the nuclear superfluid correlations have disappeared; cf. Section 3 below) the assumption of a rigid-body moment of inertia offers a better description of nuclear motion than any other estimate for $\Im$ (e.g. the estimate following from hydrodynamics of an ideal nonviscous fluid). The rigid-body estimate for the moment of inertia follows from the cranking model (see Section 2 below) for the system of independent particles in a deformed rotating nuclear potential.

In very heavy nuclei in addition to the surface energy $E_{surf}(\beta,\gamma)$ and the rotational energy $I^2\hbar^2/\{2\Im(\beta,\gamma)\}$ we have also to take into account the Coulomb energy (electrostatical repulsion of protons) $E_{Coul}(\beta,\gamma)$ that obviously favours strongly deformed shapes leading eventually to nuclear fission. Let us consider for example potential-energy surfaces expressed in terms of two parameters, the fissionability parameter

$$x = \frac{E_{Coul.}(0,0)}{2\,E_{Surf}(0,0)} = \frac{\frac{3}{5}\,\frac{e^2\,Z^2}{r_o\,A^{1/3}}}{2.\,b_{Surf}\,A^{2/3}} \approx \frac{1}{50}\,\frac{Z^2}{A} \qquad (6)$$

and the rotation parameter

$$y = \left\{ \frac{(\hbar I)^2}{2\Im(0,0)} \Big/ E_{Surf}(0,0) \right\} = \frac{\hbar^2\,I^2}{\frac{2}{5}\,A\,M\,R_o^2 \cdot b_{Surf}\,A^{2/3}} \approx 2\,I^2/A^{7/3} \qquad (7)$$

In the above formulae the expressions for $E_{Coul}(0,0)$, $E_{Surf}(0,0)$ and $\Im(0,0)$ correspond to spherical shape ($\beta = \gamma = 0$). They have been calculated using $b_{Surf} = 18$ MeV for nuclear radius

$$R_o = r_o\,A^{1/3} = 1.2\text{ fm}\cdot A^{1/3} \qquad (8)$$

and M denoting the nucleon mass.

The energy expansions of E_{Surf}, E_{Coul} and $\Im$ in terms of β and γ up to third order in powers of β have been suggested by Bohr and Mottelson [3].

$$E_{Surf}(\beta,\gamma) = b_{Surf}\,A^{2/3}\left(1 + \frac{\beta^2}{2\pi} - \frac{1}{21\pi}\sqrt{\frac{5}{4\pi}}\,\beta^3\cos 3\gamma + \ldots\right) \qquad (9)$$

$$E_{Coul.}(\beta,\gamma) = \frac{3}{5}\,\frac{e^2}{r_o}\,\frac{Z^2}{A^{1/3}}\left(1 - \frac{\beta}{4\pi}^2 - \frac{1}{21\pi}\sqrt{\frac{5}{4\pi}}\,\beta^3\cos 3\gamma + \ldots\right) \qquad (10)$$

$$E_{rot}(\beta,\gamma) = \frac{\hbar^2\,I^2}{2\Im(\beta,\gamma)} \qquad (11)$$

Dernière ligne de la page.

where $\Im(\beta,\gamma) = \frac{2}{5} M R_o^2 A \left\{1 - \sqrt{\frac{5}{4\pi}} \beta \cos(\gamma + 120°)\right\}$ (12)

These expansions seem to be quite appropriate when nuclei are very heavy and the fissionability parameter x is close to unity. The sum of the three terms given above expresses the total relevant nuclear energy

$$E(\beta,\gamma) = E_{Surf}(\beta,\gamma) + E_{Coul}(\beta,\gamma) + E_{rot}(\beta,\gamma)$$

$$= \text{const} + b_{Surf} A^{2/3} \left\{ \frac{(1-x)}{2\pi} \beta^2 - \frac{1}{21\pi}\sqrt{\frac{5}{4\pi}} \beta^3 (\cos 3\gamma) (1+2x) \right.$$

$$\left. + y \left[1 + \sqrt{\frac{5}{4\pi}} \beta \cos(\gamma + 120°)\right]\right\} \qquad (13)$$

The equipotential energy surfaces are illustrated in Fig. 4. Fig. 4a illustrates what happens if the nucleus rotates slowly ($y < y_{crit}$). The minimum occurs at $\gamma = 60°$ (oblate shape) while there is also a saddle point inside the γ- plane. Fig. 4b illustrates the situation of a fast rotation ($y > y_{crit}$). Here, the saddle point has moved to the oblate axis and there is no stability. Examination of formula (13) leads to the conclusion that

$$y_{crit} = \frac{21}{5} \frac{(1-x)^2}{1+2x} \qquad (14)$$

which is equivalent to

$$I = \left\{ \frac{84}{25} b_{Surf} \frac{M r_o^2}{\hbar^2} A^{7/3} \frac{(1-x)^2}{1+2x} \right\}^{1/2} = 1.4\, A^{7/6} \frac{1-x}{\sqrt{1+2x}} \qquad (15)$$

This estimate which is valid only for $(1-x) \ll 1$ may be used as a very crude estimate for the critical angular momentum at which the heavy nucleus goes to fission.

Finally, Figs. 5 and 6 illustrate the results of a more realistic description by Cohen, Plasil and Swiatecki[4] based on a concept of a rotating liquid drop of nuclear matter. Fig. 5 illustrates the region of existing rotating nuclei with respect to various types of instabilities. Fig. 6 gives the estimate for the maximum angular momentum that can be accomodated in the nucleus.

2 . Quantal orbits in a rotating nucleus.

A procedure that describes successfully the dynamical coupling between nuclear rotation as a whole and its intrinsic degrees of freedom has been formulated and developed[5,6] under the name of cranking model. This procedure turns out to account properly for the calculation of the nuclear moments of inertia and provides most probably an adequate description of nuclear behaviour at high angular momenta. Unfortunately the cranking model procedure does not provide

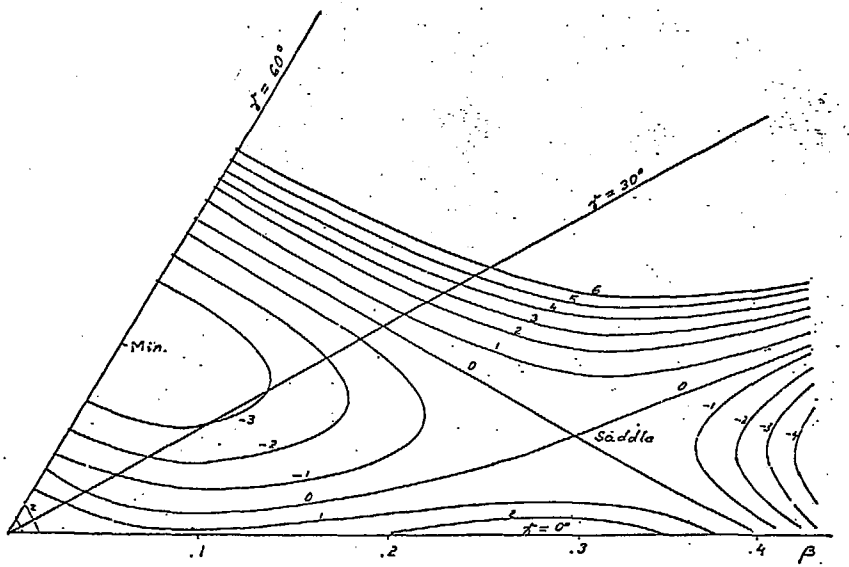

Figure 4a.

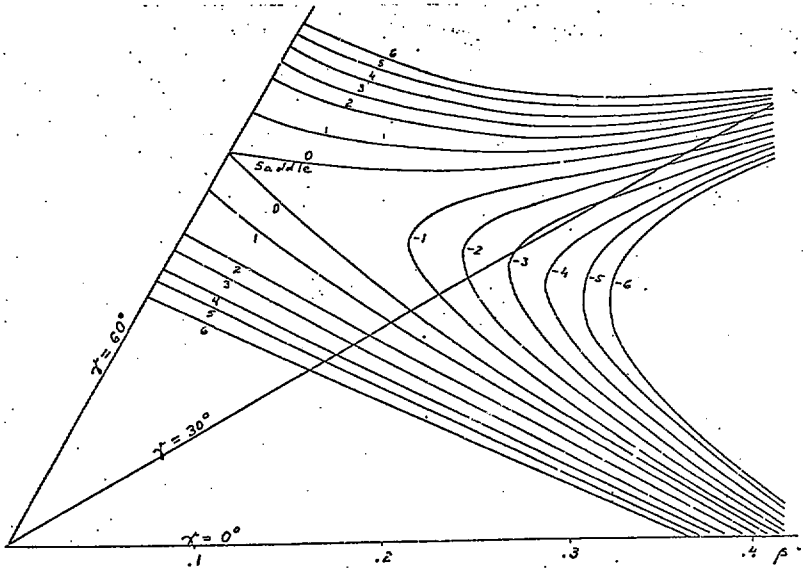

Figure 4b

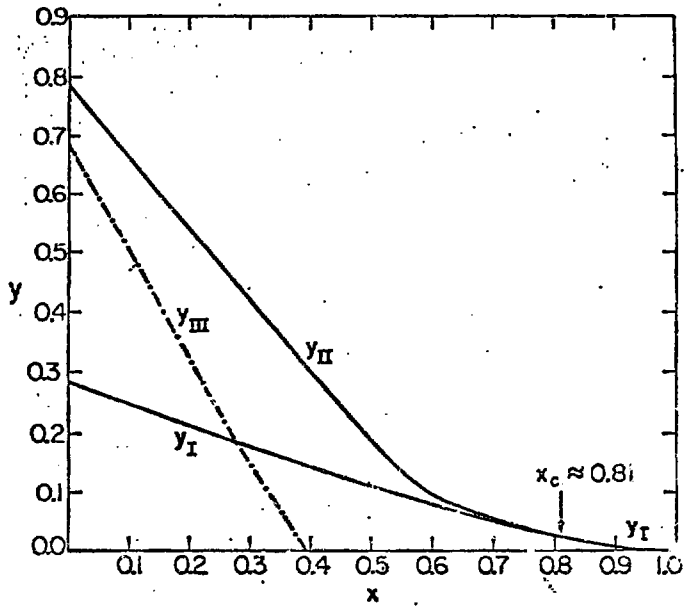
0.9
0.8
0.7
0.6
0.5
0.4
0.3
0.2
0.1
0.0
y
0.1
0.2
0.3
0.4
0.5
0.6
0.7
0.8
0.9
1.0
x
y_{III}
y_{II}
y_I
$x_c \approx 0.8i$
y_I

Figure 5

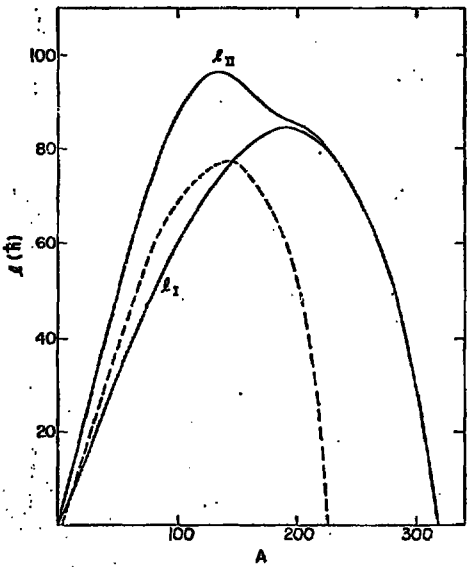

Figure 6

a derivation of the rigorous solutions in the many-body problem corresponding to nuclear rotation. We shall see that the procedure is based on a concept of an imposed rotation of the nuclear potential that is a pure classical motion. Moreover, the solutions to the corresponding cranking model Hamiltonian are not eigenfunctions of angular momentum. Finally, the rotation of a nuclear potential is imposed about an axis that is fixed in space. Thus the cranking model is not able to describe a wobbling motion of the nucleus that often accompanies the rotation. Fortunately, this last drawback of the method seems to play a minor role in the case of a fast rotation ($I >> 1$) where the wobbling correction behaves as $1/I$. In spite of all the above negative aspects of the cranking model it has been widely employed as the only method that has proved up to now to describe successfully the fast nuclear rotation.

General idea of the cranking model consists on solving the Schrödinger equation for a particle moving in an externally rotated deformed nuclear potential that is rotated with a constant angular velocity ω about an axis fixed in space. The resulting equation is of the form

$$i\hbar \frac{\partial \psi}{\partial t} = H^{\omega} \psi \tag{16}$$

where

$$H^{\omega} = H - \hbar \omega J_x \tag{17}$$

is called a cranking Hamiltonian (or a Routhian) while H is the original Hamiltonian that describes the system without rotation. It may be shown that H^{ω} may be also understood as a Hamiltonian in the rotating frame of reference. The additional term $-\hbar \omega J_x$ appearing in H^{ω} (J_x is the component on a total angular momentum vector on a rotation axis) takes care of both the centrifugal and Coriolis term known from classical mechanics to act in the rotating system. If we have a nucleonic orbit of angular momentum $\vec{J}$ in the rotating frame of reference then the Coriolis force attempts to align the "intrinsic" angular momentum $\vec{J}$ with the axis of rotation.

Another derivation of the cranking model can be given that is based on a variational principle. We simply want to minimize the energy

$$\mathcal{E} = \langle \psi | H | \psi \rangle \tag{18}$$

with the subsidiary condition of fixed angular momentum

$$I = \langle \psi | J_x | \psi \rangle \tag{19}$$

Here, again the total angular momentum I is identified with its projection on the symmetry axis. Using the method of Lagrange multipliers we have to minimize the auxiliary functional

$$E' = \langle \psi | H | \psi \rangle - \mu \langle \psi | J_x | \psi \rangle \tag{20}$$

which is then reduced to the minimisation of the auxiliary Hamiltonian

$$H^{\mu} = H - \mu J_x \tag{21}$$

The Lagrange multiplier μ is then to be determined from eq. (19) after minimisation. One can now show that the Lagrange multiplier μ is proportional to the angular velocity of rotation ω ($\mu = \hbar\omega$). Indeed differentiating the energy E with respect to I (which then defines ω) we obtain

$$\frac{dE}{dI} = \frac{d}{dI} \langle\psi|H|\psi\rangle = \frac{d\mu}{dI} \frac{d}{d\mu} \langle\psi|H|\psi\rangle =$$

$$= \frac{d\mu}{dI} \left(\left(\frac{d}{d\mu} \langle\psi| \right) H^{\mu} |\psi\rangle + \frac{d}{d\mu} \left(\mu \langle\psi|J_x|\psi\rangle \right) \right)$$

$$= \frac{d\mu}{dI} \left(\left(\frac{d}{d\mu} \langle\psi| \right) H|\psi\rangle + \langle\psi| H \left(\frac{d}{d\mu} |\psi\rangle \right) + \right.$$

$$\left. + \langle\psi| \frac{d H^{\mu}}{d\mu} |\psi\rangle + \langle\psi| J_x |\psi\rangle + \mu \frac{d}{d\mu} \langle\psi| J_x |\psi\rangle \right). \tag{22}$$

Since $|\psi\rangle$ minimizes H^{μ} we have

$$H^{\mu}|\psi\rangle = E^{\mu}|\psi\rangle \tag{23}$$

thus the first two terms in the bracket in (22) vanish

$$\left(\frac{d}{d\mu} \langle\psi| \right) H^{\mu}|\psi\rangle + \langle\psi| H^{\mu} \left(\frac{d}{d\mu} |\psi\rangle \right) = E^{\mu} \frac{d}{d\mu} \langle\psi|\psi\rangle = 0 \tag{24}$$

Moreover

$$\frac{d H^{\mu}}{d\mu} = - J_x \tag{25}$$

Hence the other two terms in eq. (22) cancel each other. We have finally :

$$\frac{dE}{dI} = \mu \tag{26}$$

However, ω can be regarded as a variable conjugate canonically to angular momentum $\hbar$ I. Hence finally

$$\omega = \frac{d E}{d(\hbar I)} = \frac{\mu}{\hbar} \tag{27}$$

and the two derivations of the cranking model coincide.

It follows from the above considerations that the cranking model procedure can be regarded as a quantal calculation in which the cranking Hamiltonian H^{ω} (the Routhian) is used as to generate the eigenfunctions $|\psi\rangle$ while the original Hamiltonian H as the true energy operator.

The transformation from H to H^{ω} with the simultaneous change of variables from I to ω is of the type of a contact transformation. Table I illustrates the conjugate relations between angular momentum I and angular velocity of rotation ω .

Table I

CONJUGATE RELATIONS

$H^{\omega} = H - \hbar\omega\ J_x$

$H^{\omega}\ |\psi> = E^{\omega}\ |\psi>$

$E = <\psi|\ H\ |\psi>$

(E = total energy; E^{ω} = total Routhian)

$I = <\psi\ |\ J_x\ |\ \psi>$

$\frac{dE^{\omega}}{d(\hbar\omega)} = -I$

single-particle version :

$h^{\omega} = h - \hbar\omega\ j_x$

$h^{\omega}|\phi_\nu> = e^{\omega}_{\nu}|\phi_\nu>$

$e_\nu = <\phi_\nu\ |h\ |\phi_\nu>$

(e_ν = s.p. energy; e^{ω}_{ν} = s.p. Routhian)

$i_\nu = <j_x>_{\nu\nu} = <\phi_\nu\ |\ j_x\ |\phi_\nu>$

$\frac{d\ e^{\omega}_{\nu}}{d\omega} = -(j_x)_{\nu\nu} = -i$ (alignment in the orbit ν)

Table II

SIGNATURE QUANTUM NUMBER

signature $r = e^{-i\pi\alpha}$	signature exponent α	angular momentum $I = \alpha \mod 2$	number of particles $A = 2\alpha \mod 2$
+1	0	0,2, 4,...	even
-1	1	1,3,5,...	even
-i	1/2	1/2,5/2,9/2,...	odd
+i	-1/2	3/2,7/2,11/2,...	odd

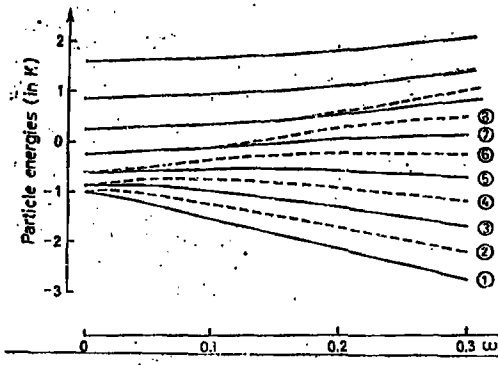

Figure 7

Figure 8

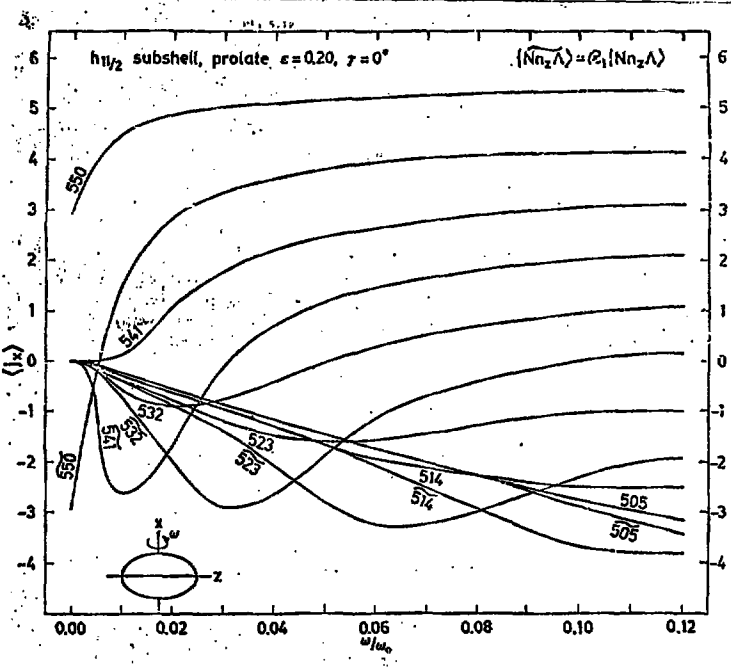

Before going to a detailed discussion of the single-particle orbits in a rotating nucleus let us still discuss the symmetry properties of the cranking Hamiltonian. In absence of the negative-multipolarity deformations (such as e.g. the octupole deformations determined by parameters $\beta_{3\mu}$) the original Hamiltonian H is symmetric with respect to the three rotations R_1, R_2 and R_3, each through an angle 180° about any of the three intrinsic axes x', y' and z' :

$$R_{\mathcal{K}} = e^{i\pi J_{\mathcal{K}}} \qquad (28)$$

with $\mathcal{K}$ = x', y' or z'. In the case of $\omega \neq 0$ (rotating nucleus; we usually assume that x' is the axis of rotation) the two operators $R_{y'}$ and $R_{z'}$ are not any more the symmetries of the cranking Hamiltonian H^{ω}. The only symmetry that remains valid is $R_{x'}$. The (complex) eigenvalues of $R_{x'}$ define a symmetry quantum number called signature. In the case of independent particles the total signature operator $R_{x'}$ turns out to be a product of the individual single-particle signatures

$$R_{x'} = \prod_{\nu} (r_1)_{\nu} \qquad (29)$$

in all occupied orbits. The signature R_1 which is an eigenvalue of $R_{x'}$, can be expressed in terms of the signature exponent α as

$$R_1 = e^{-i\pi\alpha} \qquad (30)$$

where according to eq. (28)

$$I = \alpha \bmod 2 \qquad (31)$$

Table 2 summarizes the resulting values of angular momenta I for a given signature. Fig. 7 and 8 (taken from Refs.[7] and [1]) present the single-particle Routhians e^{ω}_{ν} and alignments $i_{\nu} = (j_{x'})_{\nu\nu}$ as functions of ω for the j = 13/2 and j = 11/2 configurations, respectively. The plots correspond to certain deformation β that defines the original splitting of the multiplet at $\omega = 0$. We can see that the $\Omega = 1/2$ levels are aligned most easily (i.e. occur already for low values of ω).

It is interesting to examine the potential energy surfaces and their minima which determine the nuclear behaviour at various fixed values of angular momentum. For this purpose, one has to calculate the total energy E calculated by methods described above for fixed values of I at the mesh points in the deformation plane. The results (including also the Strutinsky renormalisation) are given in Fig. 9 (taken from ref.[1]) for the nucleus ^{160}Yb. Four following regimes of nuclear motion can be distinguished in this nucleus

1) A prolate shape of the nucleus at low angular momenta with collective rotation about an axis perpendicular to the nuclear symmetry axis. The nucleus in this region is in its superfluid phase. We shall discuss the relevant phenomena in Section 3 of the present review

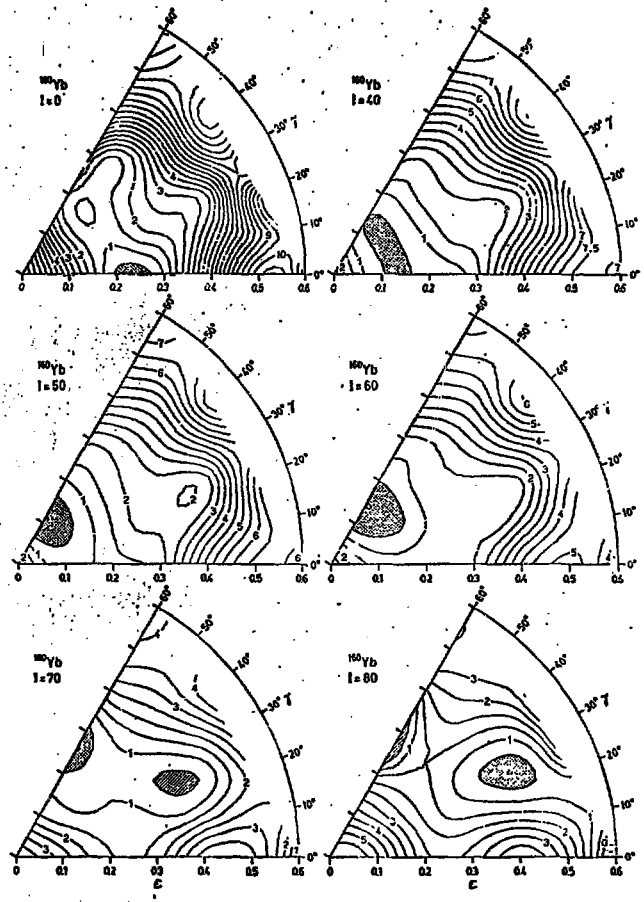

Figure 9

report.

2) A triaxial regime induced by the Coriolis and centrifugal forces which tend to align nuclear orbits with the axis of rotation and to change the shape from prolate to oblate. The superfluid correlations are probably vanishing in this region.

3) An oblate shape axially symmetric with respect to the rotation axis. Further discussion of this interesting region will be given in Section 4 of the present paper.

4) Finally a (superdeformed) triaxial and / or very elongated shape of the nucleus that occurs above the Jacobi instability point. The high-spin limit of this regime is most probably determined by nuclear fission induced by the fast rotation.

The above picture with four regimes of motion for ^{160}Yb can be of course altered for some other nuclei depending on their original deformation at I = 0 and on other nuclear parameters. Nevertheless, we may expect that fast rotation induces substantial changes of nuclear structure and many exotic effects may possibly show their presence.

Fig. 10 a, b (taken from ref.[8]) illustrates the search for the superdeformation that may be favoured by the existence of special shell effects. One can see that nuclides around Z = 66 and N = 86 may be good candidates for this search.

3. High-spin rotational bands in deformed nuclei.

In order to describe collective nuclear motion at the high (but not very high)-spin region for I, say, up to 30 in nuclei that are originally already deformed at I = 0 we have to include nuclear superfluid correlations in addition to the picture presented so far. The characteristics of nuclear superfluid correlations induced by the short-range attractive pairing force are fairly well known. They lead to the existence of the pairing gap Δ in the spectrum and the elementary excitations are of the quasiparticle type. In the simplest version of the calculation the quasiparticle energy is given by

$$\mathcal{E}_\nu = \sqrt{(e_\nu - \lambda)^2 + \Delta^2} \qquad (32)$$

where $e_\nu - \lambda$ denotes the single particle energy calculated relative to the Fermi energy λ in a given nucleus. When we want to generate wavefunctions in a rotating nucleus we have to replace the Hamiltonian H by the Routhian H^ω. It turns out that the relation (32) is not valid anymore (unless $\omega = 0$) and the quasiparticle energies have to formed from a more complicated system of matrix equations including the pairing field.

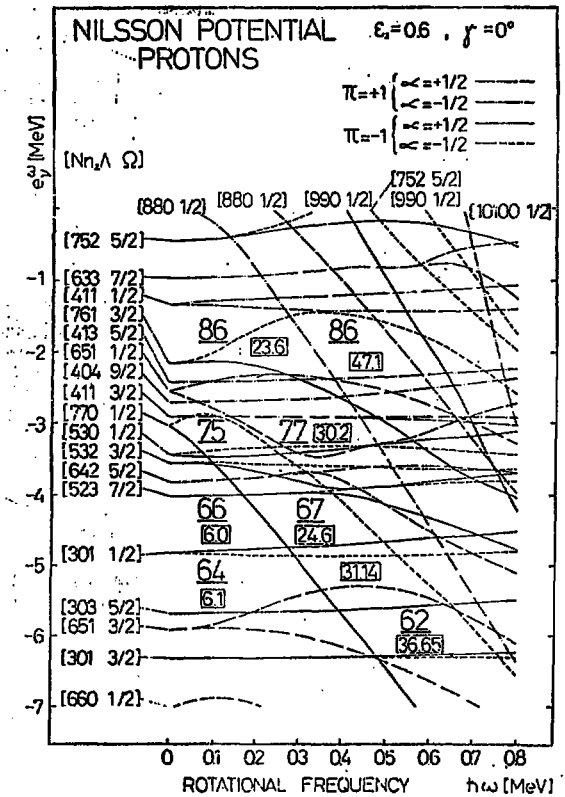
NILSSON POTENTIAL ε_4=0.6 , γ =0°
PROTONS
π=+1 α=+1/2 α=-1/2
π=-1 α=+1/2 α=-1/2
[Nn$_z$Λ Ω]
e^{ω}_{ν} [MeV]
[752 5/2]
[633 7/2]
[411 1/2]
[761 3/2]
[413 5/2]
[651 1/2]
[404 9/2]
[411 3/2]
[770 1/2]
[530 1/2]
[532 3/2]
[642 5/2]
[523 7/2]
[301 1/2]
[303 5/2]
[651 3/2]
[301 3/2]
[660 1/2]
[880 1/2]
[880 1/2]
[990 1/2]
[752 5/2]
[990 1/2]
[1000 1/2]
86
23.6
86
47.1
75
77
30.2
66
6.0
67
24.6
64
6.1
31.4
62
36.6.5
0 01 02 03 04 05 06 07 08
ROTATIONAL FREQUENCY ħω [MeV]

Figure 10a

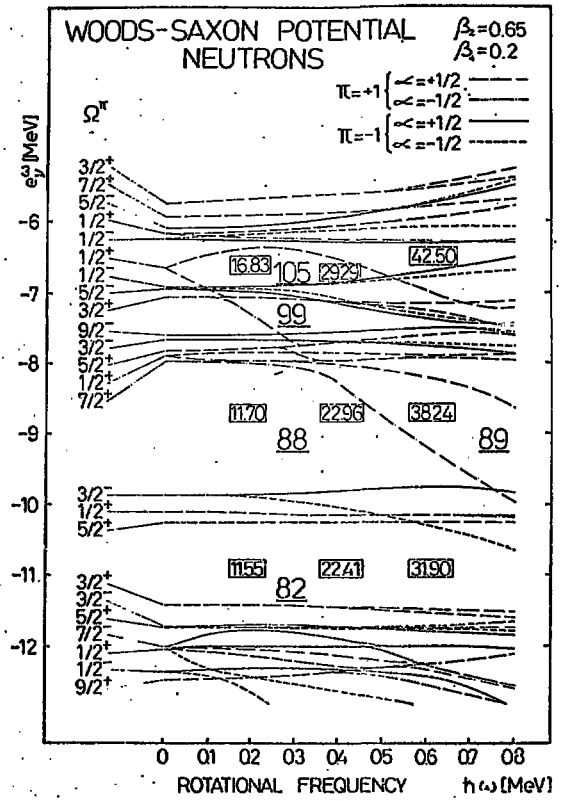
WOODS-SAXON POTENTIAL
NEUTRONS
β₂=0.65
β₄=0.2
π=+1 α=+1/2
α=-1/2
π=-1 α=+1/2
α=-1/2
Ω^π
e'_ω [MeV]
3/2+
7/2+
5/2+
1/2+
1/2-
1/2+
1/2-
5/2-
3/2+
9/2-
3/2-
5/2+
1/2+
7/2+
3/2-
1/2+
5/2+
3/2+
3/2-
5/2+
7/2-
1/2+
1/2-
9/2+
16.83
105
29.29
42.50
99
11.70
22.96
38.24
88
89
11.55
22.41
31.90
82
-6
-7
-8
-9
-10
-11
-12
0
01
02
03
04
05
06
07
08
ROTATIONAL FREQUENCY
ħω [MeV]

Figure 10b

$$\begin{pmatrix} v^{\omega} & \Delta \\ -\Delta^{*} & -v^{\omega *} \end{pmatrix} \begin{pmatrix} A \\ B \end{pmatrix} = \mathcal{E}_i \begin{pmatrix} A \\ B \end{pmatrix} \qquad (33)$$

Faire la frappe à l'intérieur du cadre bleu à nouvelle marge

(numerous original references to these equations can be found for example in refs.9, 10 or 11) where v^{ω} denotes a selfconsistent Hartree-Fock Hamiltonian (taken in a rotating frame of reference and relative to the Fermi energy multiplied by the number of particles) while Δ is a pairing gap in a rotating system. These equations when treated fully selfconsistent are called Hartree-Fock-Bogolyubov (HFB) equations. When the selfconsistency is not fully taken into account (i.e. when the potential appearing in v^{ω} and the pair field Δ are not calculated from the original two-body force but instead assumed ad hoc) it would be perhaps more modest to call them the independent quasiparticle equations in a rotating nuclear field. The solution of these equations for the eigenvalues $\mathcal{E}_i$ enable to plot them as functions of angular velocity ω. In this way the widely used plots of Bengtsson and Frauendorf are obtained[12].

In fact, equations (33) contain twice as many solutions relative to the number of the physical degrees of freedom. In the absence of rotation ($\omega = 0$) it is easy to distinguish between the physical solutions (32) and the unphysical ones ($\mathcal{E}_{\nu} = -\sqrt{(e_{\nu} - \lambda)^2 + \Delta^2}$). In the region of $\omega \neq 0$ some of the solutions originally positive become negative and vice versa. We may call "physical" those solutions $\mathcal{E}_i(\omega)$ that can be continuously connected to the positive solutions at $\omega = 0$. Fig. 11 illustrates the Bengtsson-Frauendorf plot for the nucleus ^{160}Yb (from ref. 13). One of the most striking features of this plot is the rapid change of the directions in the lowest two curves at around $\omega = 0.22$ MeV/ħ. According to the equation

$$\frac{d\,\mathcal{E}_{\nu}^{\omega}}{d(\hbar\omega)} = -i \qquad \text{(cf. Table 2)}$$

this corresponds to the rapid negative change in i (i.e. alignment of angular momentum I) proportional to the change in slope. However, the levels denoted A.B. represented by two lower curves correspond to the two quasiparticle excitation. Consequently, these two unphysical levels (not shown in the figure) represent a positive change in i, i.e. the rapid increase in angular momentum. In fact, this change (which is also accompanied by some negative jumps in angular velocity ω) corresponds to a crossing of two bands and the relevant rearrangement in the quasiparticle vacuum. This is then the explanation of the back-bending effect discovered experimentally by Johnsson, Ryde and Hjorth in 1970 in Stockholm [14]. It is now understood as a crossing of a lowest two-quasiparticle band (called Stockholm band) with the ground-state rotational band. Fig. 12 illustrates the double backbending plot (moment of inertia $\mathcal{J}$ vs. $(\hbar\omega)^2$) in ^{156}Er [15] while Fig. 13 - the prediction for nuclei ^{237}Np and ^{224}Th [16]. Generally

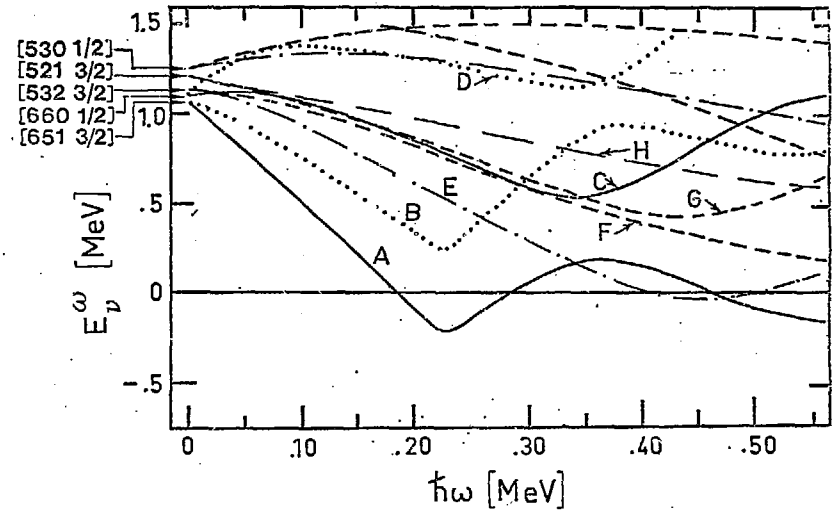
[530 1/2]
[521 3/2]
[532 3/2]
[660 1/2]
[651 3/2]
1.5
1.0
.5
0
-.5
E_ν^ω [MeV]
A
B
C
D
E
F
G
H
0
.10
.20
.30
.40
.50
$\hbar\omega$ [MeV]

Figure 11

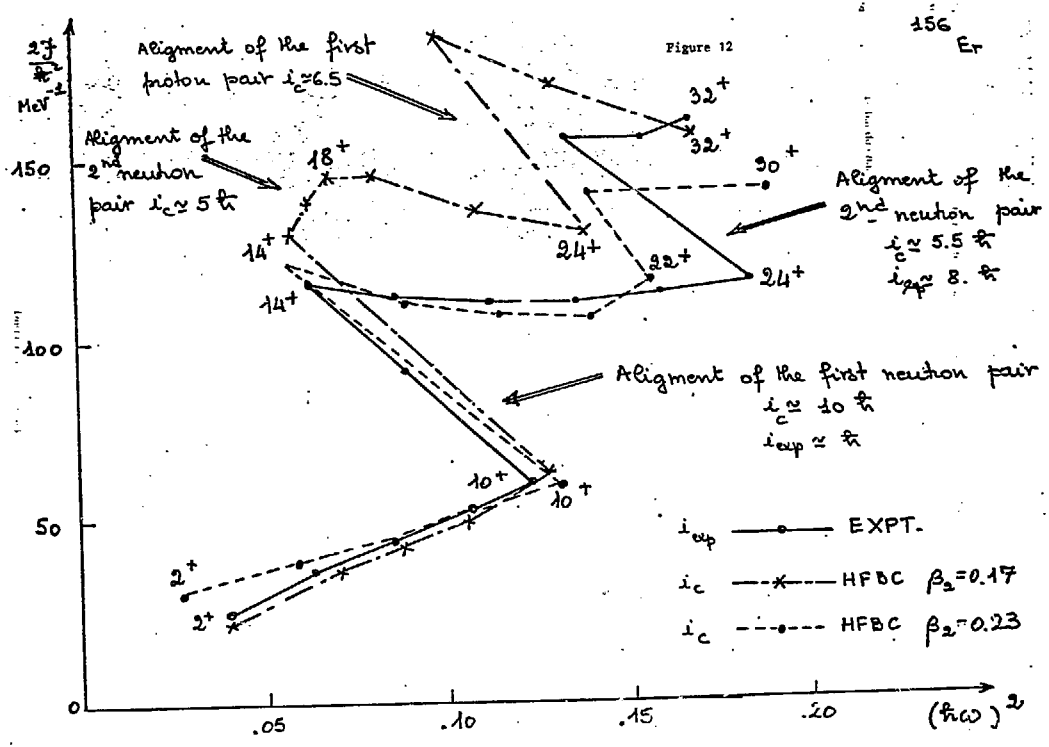
156 Er
Figure 12
Alignment of the first proton pair i_c≃6.5
Alignment of the 2nd neutron pair i_c≃ 5 ħ
Alignment of the 2nd neutron pair
i_c≃ 5.5 ħ
i_{exp}≃ 8. ħ
Alignment of the first neutron pair
i_c≃ 10 ħ
i_{exp}≃ ħ
i_{exp} EXPT.
i_c HFBC β_2=0.17
i_c HFBC β_2=0.23
$\frac{2\mathcal{J}}{\hbar^2}$ MeV^{-1}
150
100
50
0
.05
.10
.15
.20
$(\hbar\omega)^2$
32+
32+
30+
24+
22+
24+
18+
14+
14+
10+
10+
2+
2+

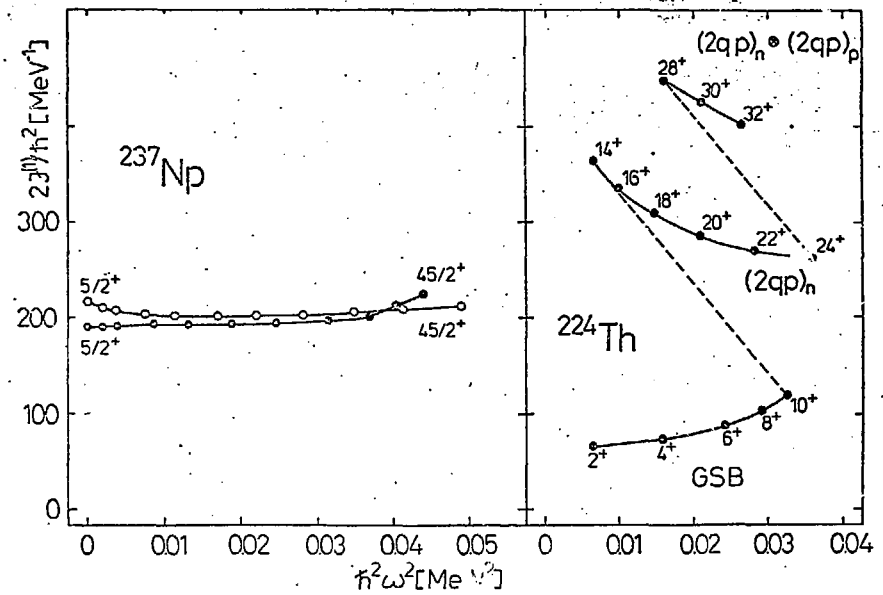
$2\mathcal{J}^{(1)}/\hbar^2$[MeV^{-1}]
300
200
100
0
^{237}Np
5/2$^+$
5/2$^+$
45/2$^+$
45/2$^+$
0
0.01
0.02
0.03
0.04
0.05
$\hbar^2\omega^2$[MeV^2]
(2qp)$_n$ ⊗ (2qp)$_p$
28$^+$
30$^+$
32$^+$
14$^+$
16$^+$
18$^+$
20$^+$
22$^+$
24$^+$
(2qp)$_n$
^{224}Th
10$^+$
8$^+$
6$^+$
4$^+$
2$^+$
GSB
0
0.01
0.02
0.03
0.04

Figure 13

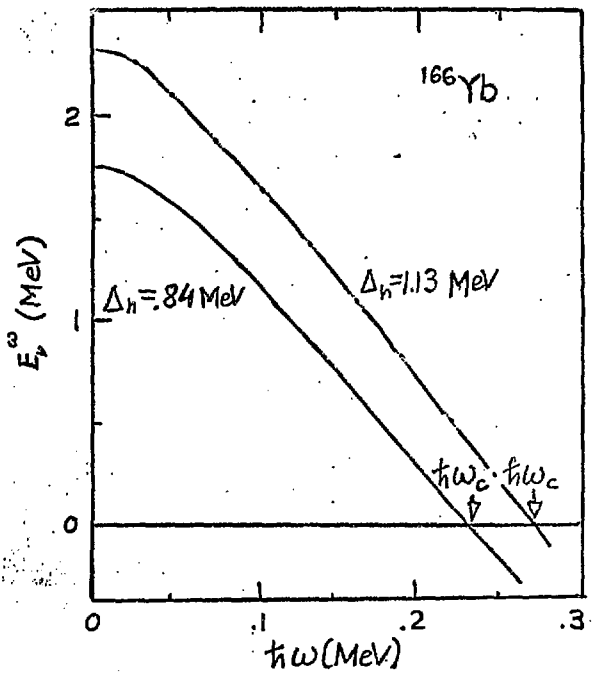
166Yb
2
1
0
E_ν^ω (MeV)
Δ_n=.84 MeV
Δ_n=1.13 MeV
$\hbar\omega_c$
$\hbar\omega_c$
0
.1
.2
.3
$\hbar\omega$(MeV)

Figure 14

we do not expect much of the back-bending behaviour in Actinide nuclei (except for some special cases). The exotic nucleus ^{224}Th, for example, should exhibit a very strong double back-bending as predicted by the theory [16].

Fig. 14 shows schematically the dependence ox the crossing frequency ω^* on the pairing force strength (and thus on energy gap Δ). This figure could be taken as the basis of the discovery by Garrettet al. [17] that the crossing frequency ω^* is generally lower in odd-A nuclei as compared to the even-even ones. Few important exceptions from this rule (illustrated on Fig. 15, [18]) concerning the oblate orbits may be an indication of an existence of a new component in the nucleon-nucleon force (e.g. quadrupole - pairing) that causes different sensitivity of some orbits with respect to the pair field Δ [18]. Fig. 16 illustrates the dependence of angular momentum I on the angular velocity ω found experimentally [19] in ^{168}Hf. A remarkable fact in this picture is a linear dependence of I on ω in a rather large interval of I (say, from I = 18 to I = 34ℏ). Moreover, the straight line can be seen to go through the origin of the coordinate system. Before analysing the implications of this remarkably simple linear dependence let us first discuss the possible definitions of nuclear moments of inertia [20]. We can define $\mathfrak{J}$ as the ratio of angular momentum I to angular velocity ω . The resulting moment of inertia

$$\mathfrak{J}^{(1)} = \frac{\hbar}{2}\left(\frac{dE}{dI^2}\right)^{-1} = \hbar\ \frac{I}{\omega} \qquad (34)$$

("kinematical" moemnt of inertia) is labelled with superscript (1) since it involves a first-order derivative of energy E with respect to I^2. The other possible quantity ("dynamical" moment of inertia) may be related to the curvature in the yrast line :

$$\mathfrak{J}^{(2)} = \hbar^2\left(\frac{d^2E}{dI^2}\right)^{-1} = \hbar\ \frac{dI}{d\omega} \qquad (35)$$

It involves a second-order derivative of energy E with respect to angular momentum I. Now, the two moments are related by the relation :

$$\mathfrak{J}^{(2)} = \mathfrak{J}^{(1)} + \omega\ \frac{d\mathfrak{J}^{(1)}}{d\omega} \qquad (36)$$

Now,let us come back to Fig. 16. The long linear part in the curve of I vs ω going through the origin means that

$$\mathfrak{J}^{(1)} = \mathfrak{J}^{(2)} = \text{const} \qquad (37)$$

independent roughly on ω . Since it has been known already that the main reason for the change in moment of inertia (at least at low spins) comes mainly from the change in the pairing one can conclude that perhaps the pairing correlations have already collapsed for I > 18 in ^{168}Hf.

$$i(\omega) = I(\omega) - I_g(\omega)$$

aligned angular momentum

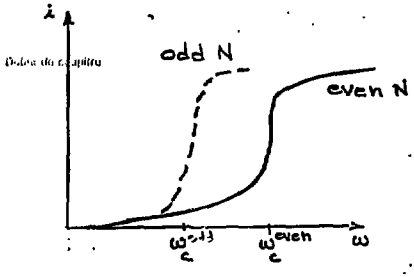

$$\delta(\hbar\omega_c) \simeq 0.07 \text{ MeV}$$

20% to 25% decrease in Δ, for odd N where normal-parity state is blocked.

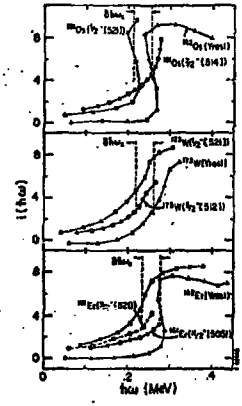

Important exceptions from the above rule. (cf. J.D. Garrett et al. [18])

Figure 15

Figure 16

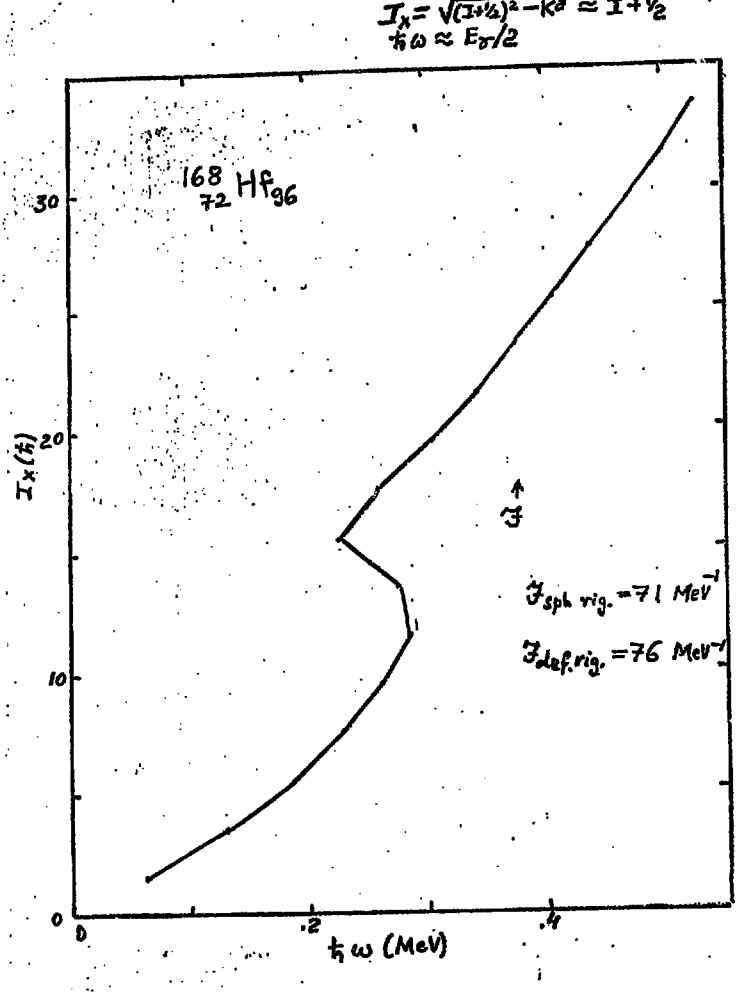
$I_x = \sqrt{(I+1/2)^2 - K^2} \simeq I + 1/2$
$\hbar\omega \approx E_\gamma/2$
$^{168}_{72}Hf_{96}$
30
20
10
0
$I_x(\hbar)$
0
.2
.4
$\hbar\omega$ (MeV)
$\mathcal{J}$
$\mathcal{J}_{sph\ rig.} = 71\ MeV^{-1}$
$\mathcal{J}_{def.rig.} = 76\ MeV^{-1}$

Figure 17

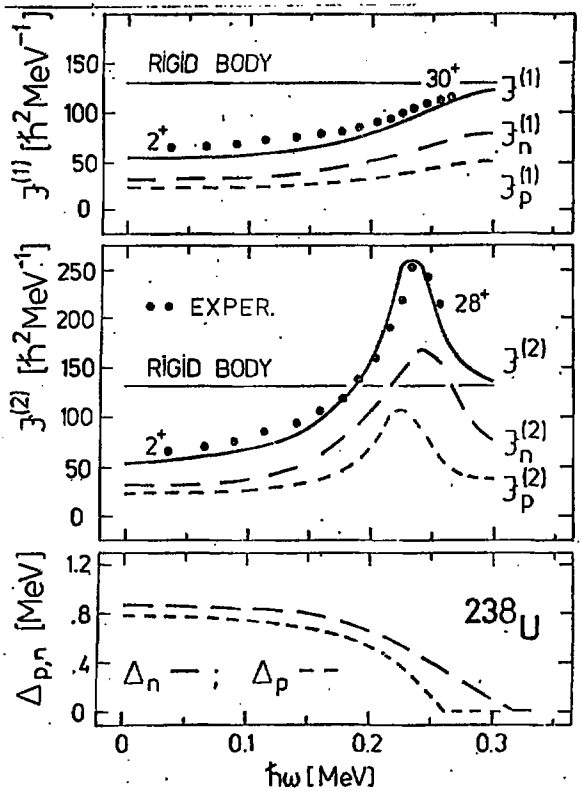

This conclusion is highly tentative, nevertheless the simple dependence of I on ω in ^{168}Hf deserves attention.

Fig. 17 shows the observed and calculated two moments of inertia $\mathcal{J}^{(1)}$ and $\mathcal{J}^{(2)}$ (taken from calculation by Dudek et al.[21]) in ^{238}U together with the calculated values of the pairing gap Δ. All the curves are plotted versus ω. It has been suggested by Bohr and Mottelson[20] that when the pairing correlations are about to be destroyed there is a region of a fast increase in angular momentum as function of ω. In this region $\mathcal{J}^{(2)}$ should be rather large. This is exactly what happens in Fig. 17 and it is remarkable that the peak in $\mathcal{J}^{(2)}$ occurs exactly in the region where the pairing gaps approach zero. Unfortunately, this exciting evidence for the pairing phase transition is also highly tentative owing to the possible existence of another explanation by means of the band crossing.

4 . Complete alignment in axially symmetric nuclei (mostly oblate or spherical)

We shall now discuss the case where the angular momentum is totally aligned along the nuclear symmetry axis. Such a coupling scheme has most chances to prevail in nuclei that are axially symmetric and oblate (or spherical) already at I = 0. The single-particle orbits in case of such motion are governed by the cranking Hamiltonian

$$h^{\omega} = h - \hbar \omega j_x \qquad (38)$$

However, now since j_x commutes with h and thus also with h^{ω} the eigenvalues e_ν^{ω}, e_ν and m_ν of h^{ω}, h and j_x, respectively, are related by :

$$e_\nu^{\omega} = e_\nu - \hbar \omega m_\nu \qquad (39)$$

In this situation, the increase in angular velocity of the motion does not modify any more the orbits and the system can pick up angular momentum only through a rearrangement in the population of various orbits. It is specially convenient in this case to consider a plane with coordinates (m,e) where the pairs (m_ν e_ν) can be represented as discrete points. The minimisation of

$$H^{\omega} = \sum_\nu h_\nu^{\omega} \qquad (40)$$

is, in this case, reduced to the proper choice of the population in the nuclear orbits. In order to create as much angular momentum as possible with the least possible energy loss one has to populate those orbits, i.e. those points in the (m,e) - plane that lie below a sloping Fermi surface represented by a straight line

Figure 18

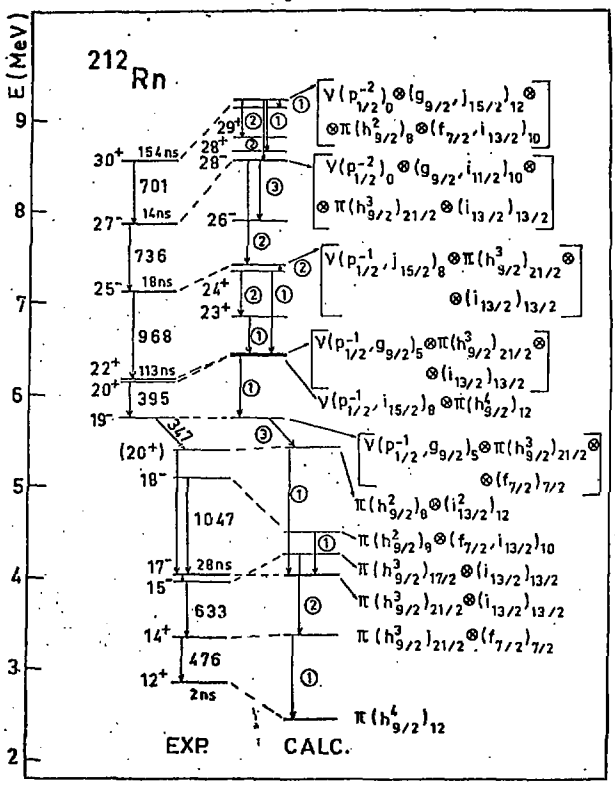
E (MeV)
212 Rn
9
8
7
6
5
4
3
2
30+ 154ns
701
14ns
27-
736
18ns
25-
968
113ns
22+
20+
395
19-
347
(20+)
18-
1047
28ns
17-
15
633
14+
476
12+
2ns
29+
28+
28-
26-
24+
23+
EXP.
CALC.
V(p-2 1/2)0 ⊗ (g9/2, i15/2)12 ⊗ π(h2 9/2)8 ⊗ (f7/2, i13/2)10
V(p-2 1/2)0 ⊗ (g9/2, i11/2)10 ⊗ π(h3 9/2)21/2 ⊗ (i13/2)13/2
V(p-1 1/2, j15/2)8 ⊗ π(h3 9/2)21/2 ⊗ (i13/2)13/2
V(p-1 1/2, g9/2)5 ⊗ π(h3 9/2)21/2 ⊗ (i13/2)13/2
V(p-1 1/2, i15/2)8 ⊗ π(h4 9/2)12
V(p-1 1/2, g9/2)5 ⊗ π(h3 9/2)21/2 ⊗ (f7/2)7/2
π(h2 9/2)8 ⊗ (i2 13/2)12
π(h2 9/2)8 ⊗ (f7/2, i13/2)10
π(h3 9/2)17/2 ⊗ (i13/2)13/2
π(h3 9/2)21/2 ⊗ (i13/2)13/2
π(h3 9/2)21/2 ⊗ (f7/2)7/2
π(h4 9/2)12

$$e = \mu' m + \lambda$$

where $\mu = \hbar\omega$ determining the slope in this line is related to the angular velocity ω. However, ω, has only a formal meaning, since there is no collective rotation in this case.

The irregular character of the sequence of levels of different nature may lead to the existence of isomeric states (yrast traps) characterised by high angular momenta of the states. The high-spin isomers are then a characteristic feature of this region of nuclides[22].

Fig. 18 taken from[23] illustrates the resulting spectrum in ^{212}Rn obtained by the method described above. The calculation is compared with experiment. One can easily see that the agreement of the calculation with the observed energy levels as well as for the occurence of the high-spin isomers is remarkable [23].

It is interesting to analyse the possible collective excitations that can be created in the high-spin states of the type discussed above. We shall give few examples of the possible collective modes that can play a certain role in establishing the nuclear coupling scheme just above the yrast line.

One possible mode is the gamma-vibration (i.e. non axial change of shape corresponding to a dynamical change in the deformation parameter γ). This type of vibration carries ± 2 units of angular momentum. The $\Delta I = -2$ mode may lead to the erosion of yrast traps [24] and the $\Delta I = +2$ modes may form a vibrational band raising just above the yrast line. The bands of this type would compete with the rotational bands that correspond to a rotation of an oblate nucleus about the axis perpendicular to its symmetry axis [20,25,26]. These two types of excitations can be derived from the dynamical variations of nuclear shape corresponding to the dynamical changes in nuclear shape of the quadrupole type (γ^{22} and γ^{21} modes).

Fig. 19 illustrates the nuclear response-functions estimated in ^{158}Yb at small oblate deformation [23]. It can be seen that the calculation predicts much more strength for the rotation as compared to the γ-vibrations which appear to be almost non collective.

Finally, a very interesting mode that has been observed in the nuclear states at high-spin is the giant resonance [27,28]. This type of excitations are presently intensively investigated both in experiments and theory (see e.g.[29]). Fig. 20 illustrates the predictions of the interesting splitting in the giant-resonance energy caused by the deformation and rotation under the assumption of its dipole-isovector character[30] (See also[31,32]). Another interesting evidence (which is not available yet) would be provided by the angular distribution of the gamma rays deexciting the giant resonance in a fast rotating nucleus[28].

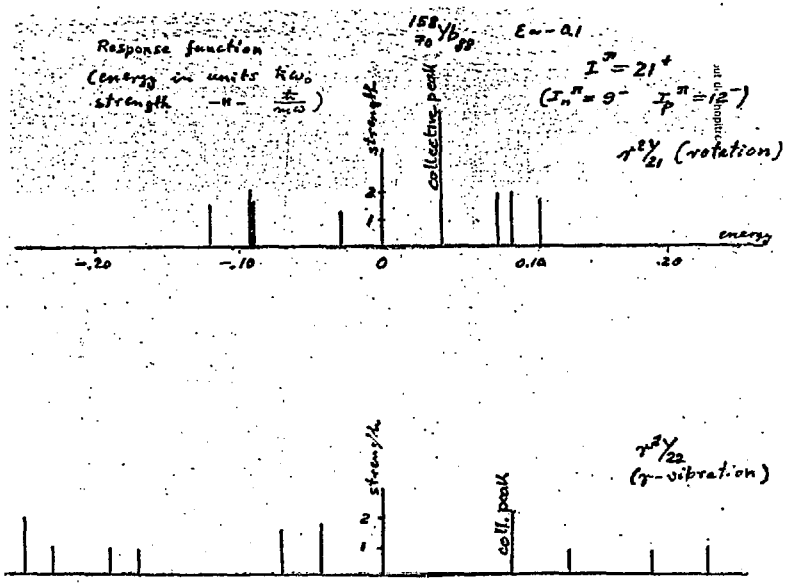
Response function
(energy in units $\hbar\omega_0$
strength $-\pi - \frac{\pm}{2m\omega}$)
$^{158}_{70}Yb_{88}$
$E\omega - 0.1$
$I^\pi = 21^+$
$(I_n^\pi = 9^-$ $I_p^\pi = 12^-)$
$\pi^2 Y_{21}$ (rotation)
collective peak
strength
energy
-.20
-.10
0
0.10
.20
$\pi^2 Y_{22}$
(γ-vibration)
coll. peak

Figure 19

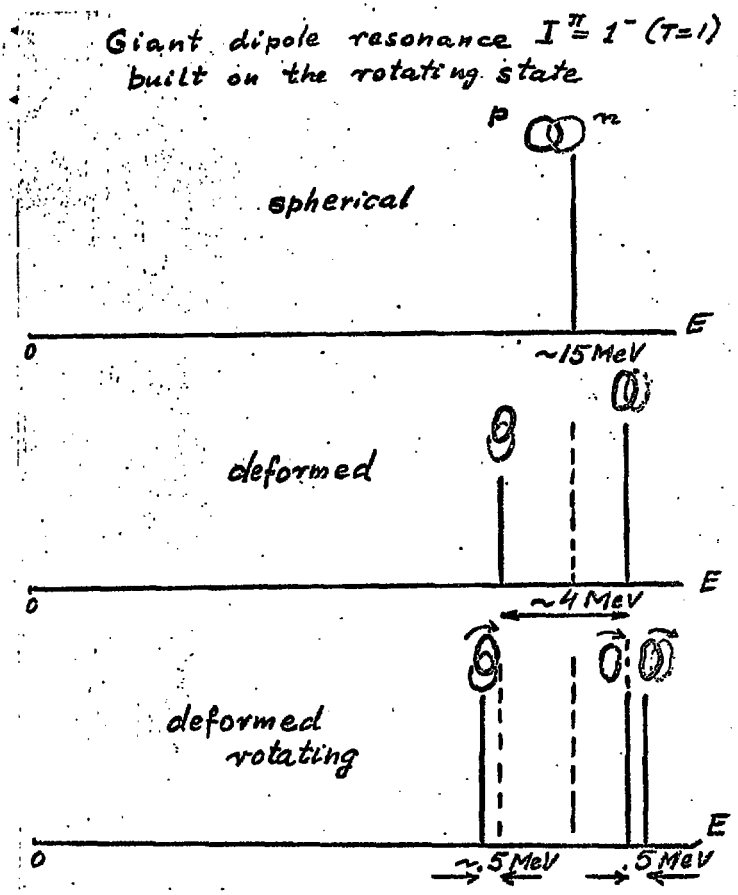
Giant dipole resonance $I^{\pi} = 1^{-}$ (T=1)
built on the rotating state
p
n
spherical
E
0
~15 MeV
deformed
E
0
~4 MeV
deformed
rotating
E
0
~.5 MeV
.5 MeV

Figure 20

In this short and simplified review on the properties of the fast rotating nuclei we have given only a very schematic picture emphasizing mostly some theoretical aspects of the problem. It is needless to add that our discussion has been highly incomplete. Fortunately, in an accompanying course by Henri Sergolle[33] some of the beautiful and exciting experiments on the fast rotating nuclei have been presented (see also Refs. 34 and 35).

We have based our discussion on a basic concept in nuclear structure of the independent (or almost independent) nucleons moving in a given nuclear potential field. In fact, we never worried in our considerations whether the assumed nuclear potential really corresponds to the actual distribution of nucleons that move in this potential. In other words, we have only occasionally taken into account the rich consequences of the selfconsistency conditions that have proved to play such an important role in understanding various aspects of nuclear dynamics. In this context, we would like to mention especially the works of the groups in Bordeaux and Orsay (see e.g. refs. 36 to 39). Some of these aspects have been also discussed in a lecture course by Michèle Meyer [40]. One may hope that the Hartree-Fock and Hartree-Fock-Bogolyubov methods would soon become basic and commonly used tools in the investigation of the high-spin states in atomic nuclei.

References

1. C.G. Andersson, S.E. Larsson, G. Leander, P. Möller, S.G. Nilsson, I. Ragnarsson, S. Åberg, R. Bengtsson, J. Dudek, B. Nerlo-Pomorska, K. Pomorski and Z. Szymanski, Nucl. Phys. A268 (1976) 205
2. S. Chandrasekhar, Ellipsoïdal figures of equilibrium, 1969, Yale University Press, New-Heaven
3. A. Bohr and B.R. Mottelson, Nuclear Structure, Vol. 2, 1975, W.A. Benjamin Inc. Reading, London, Amsterdam and Don Mills, Ontario, Sydney, Tokyo
4. S. Cohen, F. Plasil and W.J. Swiatecki, Ann. Phys. N.Y. 82 (1974) 557
5. D.R. Inglis, Phys. Rev. 96 (1954) 1059 and 97 (1955) 701
6. A. Bohr and B.R. Mottelson, Mat. Fys. Medd. Dan. Vid. Selsk. 30 (1955) n° 1
7. I. Hamamoto, High angular momentum phenomena, a review, Nordita preprint 81/28, June 1981
8. J. Dudek, A. Majhofer, W. Nazarewicz and Z. Szymanski, Phys. Lett. B 112(1982) 1
9. A. Faessler, M. Ploszajczak and K.W. Schmid, Progr. Part. Nucl. Phys. 5 (1981) 79
10. Z. Szymanski, Fast nuclear rotation, Clarendon Press, Oxford, 1983
11. M.J.A. de Voigt, J. Dudek and Z. Szymanski, Rev. Mod. Phys. October 1983, to be published
12. R. Bengtsson and S. Frauendorf, Nucl. Phys. A327 (1979) 139
13. L.L. Riedinger, O. Andersen, S. Frauendorf, J.D. Garrett, J.J. Gaardhoje, G.B. Hagemann, B. Herskind, Y.V. Makovetzky, J.C. Waddington, M. Guttormsen and P.O. Tjom, Phys. Rev. Lett. 44 (1980) 568
14. A. Johnson, H. Ryde and S.A. Hjorth, Nucl. Phys. A179 (1972) 753
15. T. Byrski, F.A. Beck, C. Gehringer, J.C. Merdinger, Y. Schutz, J.P. Vivien, J. Dudek, W. Nazarewicz and Z. Szymanski, Phys. Lett. 102B (1981) 235
16. J. Dudek, W. Nazarewicz and Z. Szymanski, Phys. Rev. C26 (1982) 1708

17. J.D. Garrett, O. Andersen, J.J. Gaardhoje, G.B. Hagemann, B. Herskind, J. Kownacki, J.C. Lisle, L.L. Riedinger, W. Walus, N. Roy, S. Jonsson, H. Ryde, M. Guttormsen and P. Tjom, Phys. Rev. Lett. 47 (1982) 75

18. J.D. Garrett, G.B. Hagemann, B. Herskind, J. Bacelar, R. Chapman, J.C. Lisle, J.N. Mo, A. Simcock, J.C. Wilmott and H.G. Price, Phys. Lett. 118B (1982) 297.

19. R. Chapman, J.C. Lisle, J.N. Mo, E. Paul, J. Wilmott, J.R. Leslie, H.C. Price, P.M. Walker, J. Bacelar, J.D Garrett, G.B. Hagemann, B. Herskind, A. Holm and P.J. Nolan, preprint 1983

20. A. Bohr and B.R. Mottelson, Phys. Scripta, 24 (1981) 71 (Nuclei at Very High Spin -- Sven Gösta Nilsson in Memoriam, Proc. Nobel Symp. Örenäs (1980))

21 J. Dudek, W. Nazarewicz, J. Skalski, Z. Szymanski and S. Cwiok, to be published

22. A. Bohr and B.R. Mottelson, Phys. Scripta A10 (1974) 13

23. J. Dudek, J. Skalski and Z. Szymanski in preparation

24. C.G. Andersson and J. Krumlinde, Nucl. Phys. A291 (1977) 21

25. C.G. Andersson, J. Krumlinde, G. Leander and Z. Szymanski, Nucl. Phys. A361 (1981) 147

26. C.G. Andersson, R. Bengtsson, T. Bengtsson, J. Krumlinde, G. Leander, K. Neergård, P. Olanders, J.A. Pinston, I. Ragnarsson, Z. Szymanski and S. Åberg, Phys. Scripta 24 (1981) 266 (Nuclei at Very High Spin -- Sven Gösta Nilsson in Memoriam, Proc. Nobel Symp. Örenäs , 1980)

27. J.O. Newton, B. Herskind, R. M. Diamond, E.L. Dines, J.E. Draper, K.H. Lindenberger, C. Schück, S. Shih and F.S. Stephens, Phys. Rev. Lett. 46 (1981) 1383

28. J.J. Gardhøje, XX Winter Meeting on Nucl. Phys., Bormio, 1982

29. P. Ring, invited talk at Conf. on High Angular Momentum Properties of Nuclei, Oak Ridge, 1982

30. Z. Szymanski and I. Ragnarsson, XIV Masurian Summer School on Nucl. Phys., Mikołajki, Poland, 1981

31. A.V. Ignatyuk and I.N. Mikhailov, Yad. Fis. 33 (1981) 919

32. K. Neergård, Phys. Lett. 110B (1982) 7

33. H. Sergolle, Lecture course delivered at this School (Ecole Joliot-Curie de Physique Nucléaire, 1983)

34. B. Haas, invited seminar at this School (Ecole Joliot-Curie de Physique Nucléaire, 1983)

35. J.P. Vivien, invited seminar at this School (Ecole Joliot-Curie de Physique Nucléaire, 1983)

36. M.J. Giannoni and P. Quentin, Phys. Rev. C21 (1980) 2060

37. M.J. Giannoni and P. Quentin, Phys. Rev. C21 (1980) 2077

38. D.M. Brink, M.J. Giannoni and M. Veneroni, Nucl. Phys. A258 (1976) 237

39. M. Baranger and M. Véneroni, Ann. Phys. (N.Y.) 114 (1978) 123.

40. M. Meyer, lecture course delivered at this School (Ecole Joliot-Curie de Physique Nucléaire, 1983).